

## Supporting Information

### **Designing Bijels formed by Solvent Transfer Induced Phase Separation with Functional Nanoparticles**

*Stephen Boakye-Ansah<sup>1</sup>, Matthew Schwenger<sup>1</sup>, Martin F. Haase<sup>1</sup>,*

<sup>1</sup>Rowan University, Henry M. Rowan College of Engineering, Glassboro, NJ 08028 USA.

**Supplementary Note 1: Calculation of the amounts of organofunctional silane added to tune the wettability of silica nanoparticles**

**Supplementary Note 2: Acid-Base titrations and calculations on the functionalized particles**

**Supplementary Note 3: Characterization of STrIPS bijel fibers.**

**Supplementary Note 4: Nucleated STrIPS fibers formed by addition of C<sub>16</sub>TAB to the ternary mixtures**

**Supplementary Note 5: Surface pore and Domain size characterization of ASNP-STrIPS bijels**

**Supplementary Note 6: Control of excess nanoparticles at the surface of ASNP-STrIPS bijels**

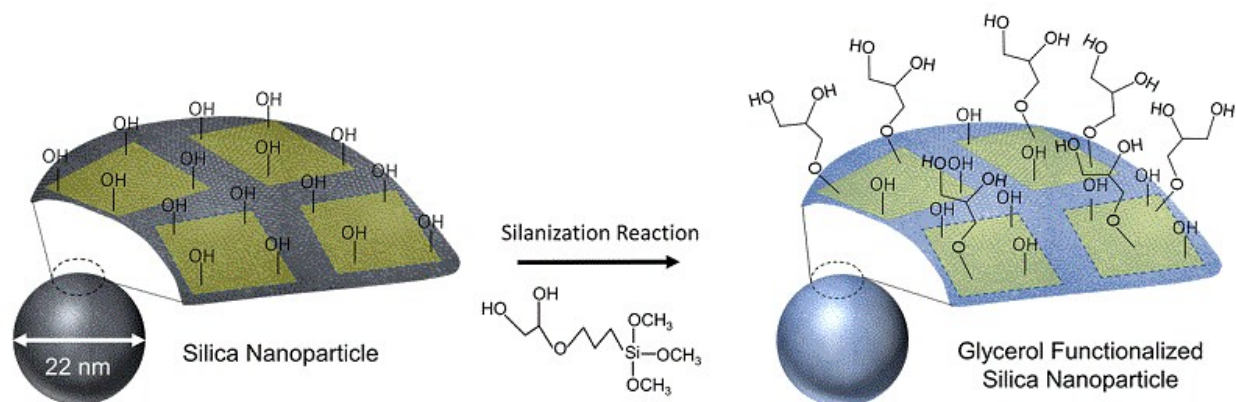
**Supplementary Note 7: Surface Charge Measurements of glycerol functionalized silica nanoparticles particles.**

**Supplementary Note 8: Effect of glycerol density and surfactant concentration on STrIPS bijel formation.**

**Supplementary Note 9: Dye adsorption on crosslinked bijel scaffolds after fluid remixing**

## Supplementary Note 1: Calculation of the amounts of organofunctional silane added to tune the wettability of silica nanoparticles

The schematic in Supplementary Figure 1 depicts the approximated number of silanol groups per nm<sup>2</sup>, based on which calculations are made to functionalize the silica nanoparticles (SNPs) (22 nm) with the various organofunctional silanes.<sup>1</sup> As a demonstration we choose the silanization of 22 nm SNPs with Glycidoxypropyl trimethoxy silane (GPO), which we believe are distributed on the surface of the particles in relation to the degree of functionalization, hence, tuning their surface wettabilities.



**Supplementary Figure 1:** Depiction of silica nanoparticle spherical surface covered with silanol (Si-OH) groups. Assumption is made for 4 Si-OH groups per nm<sup>2</sup> and also, for an overall surface area of 150 m<sup>2</sup>/g. Based on this estimation, the amount of organofunctional silane molecules is added during the silanization process, resulting in a percentage coverage (degree) of the selected functional groups. In this schematic, a 22 nm silica nanoparticle is silanized with 3-glycidoxypropyl trimethoxy silane (GPO).

The following calculations provide estimations made during the silanization of the silica nanoparticles. The total number of silanol groups ( $N_{\text{SiOH}}$ ) on the silica particles is calculated as:

$$N_{\text{SiOH}} = 4 \text{ Si-OH molecules/nm}^2 \times 150 \text{ m}^2/\text{g} = \mathbf{6.0 \times 10^{20} \text{ SiOH molecules/g}}$$

Calculation is made for the total number of SiOH molecules ( $n_i$ ) (in moles per gram) by dividing  $N_{\text{SiOH}}$  by the Avogadro's number,  $N_{\text{AV}}$ :

$$n_i = N_{\text{SiOH}} / N_{\text{AV}} = 6.0 \times 10^{20} [\text{SiOH molecules/g}] / 6.0223 \times 10^{23} [\text{molecules/mol}]$$

$$= 9.963 \times 10^{-4} \text{ mol/g}$$

Hence, mass of organofunctional molecules ( $m_{\text{silane}}$ ) required for silanization is calculated as:

$$(m_{\text{silane}}) = n_i [\text{molecules/mol}] \times \text{molar mass } (M_i [\text{g/mol}])$$

$$m_{\text{silane}} = 9.963 \times 10^{-4} [\text{mol/g}] \times M_i [\text{g/mol}];$$

Where  $M_i$  is the molar mass of the chosen organofunctional silane.

The added mass ( $\Delta m$ ) of silica nanoparticles (SNPs) to the reaction vessel is calculated as:

$$\Delta m_{\text{SNPs}} = \Delta V_{\text{SNPs}} \times \rho_{\text{SNPs}} \times W_{\text{SNPs}}$$

Where  $\Delta V_{\text{SNPs}}$  is the volume ( $ml$ ) of aqueous of SNPs dispersion (*Ludox TMA*) added;  $W_{\text{SNPs}}$  is the weight fraction of SNPs in the aqueous dispersion ( $50 \text{ wt}\%$ ); and  $\rho_{\text{SNPs}}$  is the density of aqueous SNPs dispersion ( $1.23 \text{ g/ml}$ , *Ludox TMA*).

Hence, the amount of organofunctional groups ( $n_{\text{silane}}$ ) (in mols) required to tailor the wettability of the SNPs can be calculated as

$$n_{\text{silane}} = m_{\text{silane}} \times \Delta m_{\text{SNPs}} / M_i \times S$$

where  $S$  = fraction of organofunctional silane on the surface of nanoparticles, represented in this calculation as  $0.2$ ,  $0.4$  and  $0.6$ , which results in 20%, 40% and 60% degrees of functional densities). Therefore, the added mass for the degree of organofunctional silanes required ( $\Delta m_{\text{silane}}$ ) can be calculated as:

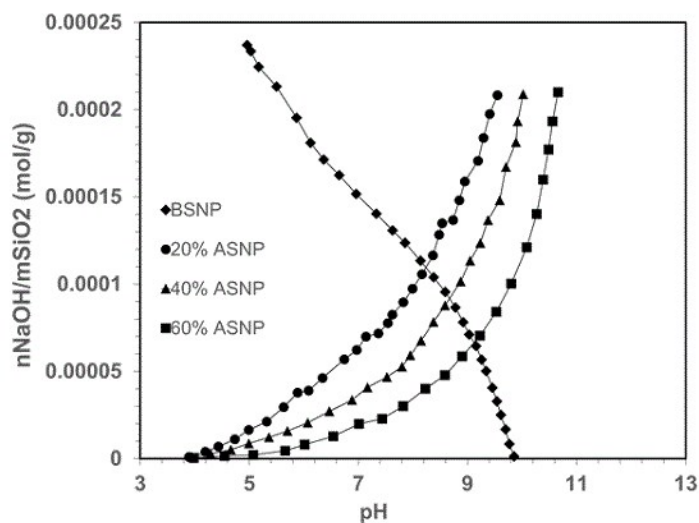
$$\Delta m_{\text{silane}} = n_{\text{silane}} \times M_i$$

And lastly, the volume of organofunctional silanes needed is:

$$\Delta V_{\text{silane}} [\text{ml}] = \Delta m_{\text{silane}} / \rho_{\text{silane}}$$

## Supplementary Note 2: Acid-Base titrations and calculations on the functionalized particles

Acid base titrations are used to characterize the efficiency of the silanization reactions performed on the acrylate functionalized silica nanoparticles (ASNPs) functionalized at 20%, 40% and 60% acrylate densities. The curves are derived from the addition of molar concentrations of NaOH and HCl for acrylate and bare silica nanoparticles respectively, which alters the pH of the titration solutions.



**Supplementary Figure 2:** Acid base titrations on silica nanoparticles. Addition of molar concentrations of hydroxyl ions ( $\text{OH}^-$ ) results in the alteration of the pH of dispersed acrylate functionalized silica nanoparticles, tagged 20%-ASNP, 40%-ASNP and 60%-ASNP. A stock solution of 1M NaOH is used to titrate the acrylate silica nanoparticles whereas 1M HCl is used for the bare silica nanoparticles.

At a chosen pH interval,  $\alpha_{100}$  is designated for the slope on the curve resulting from acid base titrations of bare silica nanoparticles (BSNPs), whereas  $\alpha_{80}$ ,  $\alpha_{60}$  and  $\alpha_{40}$  are correspondingly designated for 20%-ASNPs, 40%-ASNPs and 60%-ASNPs respectively. The real densities of adsorbed organofunctional silanes are derived thus wise:

$[1 - \alpha_{80}]$ ,  $[1 - \alpha_{60}]$ , and  $[1 - \alpha_{40}]$  for each of the acrylate groups, which are used to plot for the *calculated densities* (in Note 1, above) versus real densities  $[1 - \alpha_x]$ .

### Supplementary Note 3: Characterization of STRIPS bijel fibers.

Confocal Laser Scanning Microscopy (CLSM) images obtained from scanning at different depths of STRIPS bijel fibers fabricated with acrylated silica nanoparticles (ASNP). ASNP-bijel fibers are processed to obtain 3D reconstructions and bijel-domain size measurements. To demonstrate this, the CLSM image slices obtained from scanning the 60%-ASNP bijel fiber (in main text, Fig. 2a) are used. Supplementary Figure 3a shows the images of confocal scans at different fiber depths. Bijel domain sizes are determined by measuring the dimensions of bicontinuous channels (at multiple locations) as indicated by white lines in the magnified image at 30  $\mu\text{m}$  depth. The average of domain measurements at chosen fiber depths are used to generate Fig. 2b in main text. Supplementary Fig. 3b shows the 3D reconstructed side and front views of a 60%-ASNP STRIPS bijel fiber segment processed at different depths ( $\Delta z_i$ ).

Corresponding binary images at chosen fiber depths are used to derive the scaled oil-to-water volume ratio (in main text, Fig. 2d). Using the “adaptive thresholding” plugin for ImageJ, we convert the 2-dimensional micrographs into binary images, from which the percentage area of the corresponding oil domains ( $A_i$ ) are measured at varying depths ( $\Delta z_i$ ) of the bijel fiber (supplementary Figure 3b). Hence, the approximated fractional volume of oil ( $V_o$ ) is calculated as:  $A_1\Delta z_1 + A_2\Delta z_2 + A_3\Delta z_3 + \dots\dots\dots A_n\Delta z_n$ . The total volume of the bijel ( $V_T$ ) comprising both oil and water domains is calculated as  $A_T(\Delta z_1 + \Delta z_2 + \Delta z_3 + \dots\dots\dots \Delta z_n)$ , where  $A_T$  is the area of a selected region in chosen confocal slices. Thereby, oil-to-water-volume ratio is derived as  $V_o/V_T$  (Figure 2d in main text).

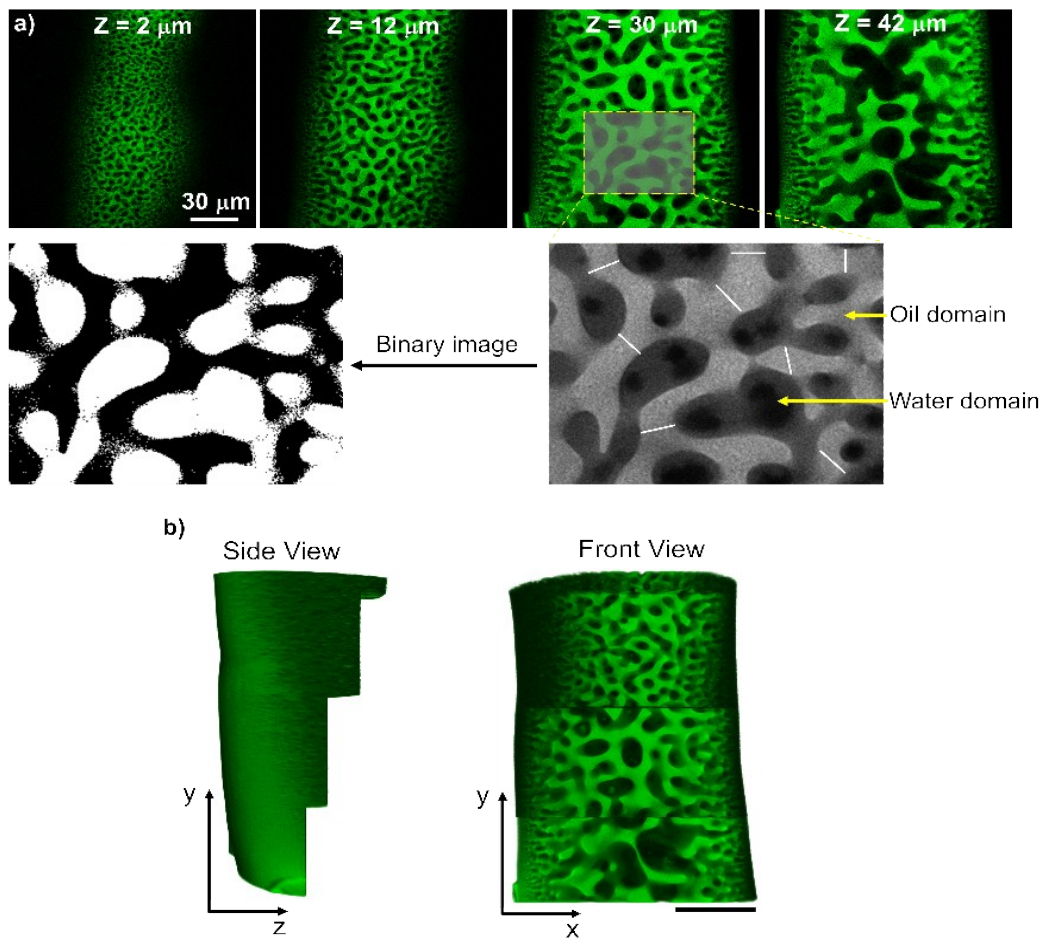
Also, to measure the volume specific surface areas of the ASNP STRIPS bijel fibers (in the main text, Figure 2a), a similar approach for measuring the surface area of previously generated STRIPS bijel fibers, as reported by Haase *et al.*,<sup>1</sup> was used. The volume specific

surface area (shown in main text, Figure 2c) is estimated as follows. Sections of the polymerized (BDA) ASNP bijel fibers are subjected to refractive-index matching by first soaking in ethanol and then in pure diethyl phthalate. Following this, a high resolution (1056 X 1056 pixel) confocal image is taken along the equatorial section of the fiber sample. The confocal images are then converted into binary images by using the “adaptive thresholding” plugin from ImageJ. A section of the equatorial binary image is first selected from the center to the surface of the fiber (~20um). The selected section is then segmented into thin strips of  $\Delta r$ . For each stripe region of fiber length ( $L$ ), the area fraction of oil ( $A_o$ ) and the perimeter of the curved interfaces ( $p(r)$ ) are determined. Based on the approximation that the bijel fibers have radially uniform internal structures, we estimate the interfacial areas ( $A(r)$ ) and volumes ( $V(r)$ ) of the polymerized bicontinuous scaffold within a thin cylindrical shell as follows:

$$A(r) = 2\pi r \cdot p(r) \text{ and } V(r) = 2\pi r L \cdot A_o.$$

The volume specific surface areas ( $As$  [ $\mu\text{m}^2/\mu\text{m}^3$ ]) of the bijel fibers (shown in main text, Figure 2c) are calculated as follows:

$$As = \frac{\sum_{r=0}^R A(r)}{\sum_{r=0}^R V(r)}$$

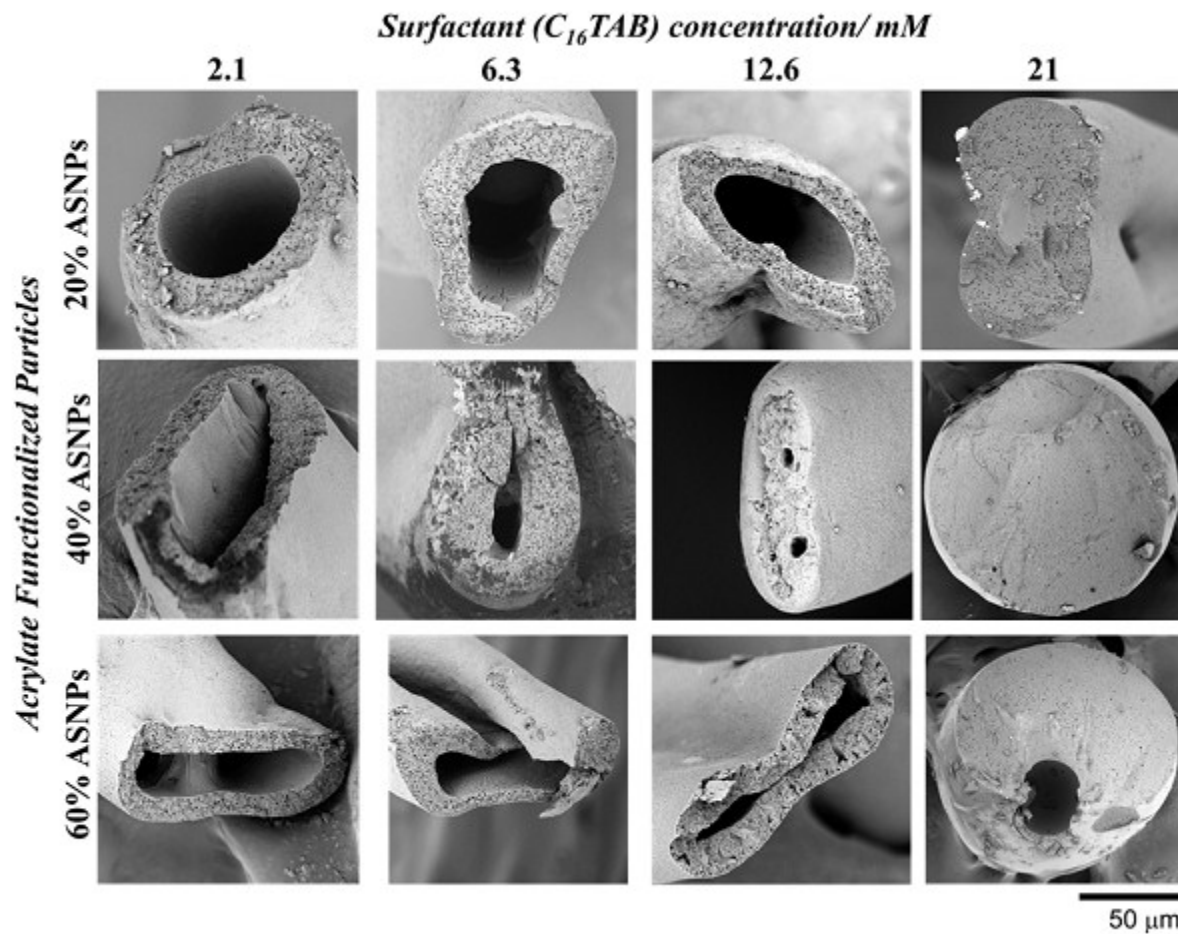


**Supplementary Figure 3:** Characterization of bijel fibers. a) Confocal laser scanning micrographs of a 60%-ASNP bijel fiber at different depths, where the oil domains are colored as green. To characterize the images, the magnified section (in gray-scale) at for example,  $\sim 30 \mu\text{m}$  fiber depth, is converted into a binary image and used to derive the domain size measurements in Fig. 2b (in main text). b) 3D confocal reconstructions of a cascading bijel fiber showing different views, as a result of processing confocal stacks in a stepwise fashion at different depths ( $\Delta z$ ). This post-processing technique is used to visualize the internal morphologies of STrIPS bijel fibers generated in Figures 2 and 4 (in main text).

#### **Supplementary Note 4: Nucleated STrIPS fibers formed by addition of C<sub>16</sub>TAB to the ternary mixtures**

STrIPS bijel fibers fabricated with ternary mixtures prepared with the surfactant, C<sub>16</sub>TAB, shows nucleated structures (supplementary Figure 4). Failure to form bicontinuous structures is attributed to the extreme hydrophobicity imparted to the acrylate particles, which likely partitions predominantly into the oil-rich phase, after interacting with long-chain C<sub>16</sub>TAB surfactants. This also contributes significantly to the hollowness of bijel fibers, as similar to previously observed results,<sup>2</sup> but are curtailed with the use of a shorter hydrocarbon chain length surfactant (C<sub>12</sub>TAB), as shown in the main text (Figure 4). Jamming of particles at the surface of the bijel fiber obstructs the transfer of solvent out of the bijel fiber, and in cases where extensive nanoparticle aggregation occurs at the bijel surface, this phenomenon is even more pronounced. We believe that this results in the “trapping” of a water-rich phase inside the bijel fibers, hence the hollowness. Also, it is likely that at high surfactant concentrations, phase inversion occurs leading the formation of an oil-in-water system, for example, at 21mM for 20% ASNPs and 12.6mM and 21mM for 40% ASNPs. Even more interesting is the formation of multiple droplets (water-in-oil-in-water emulsions) at high C<sub>16</sub>TAB concentrations (21 mM) for 60% ASNPs.

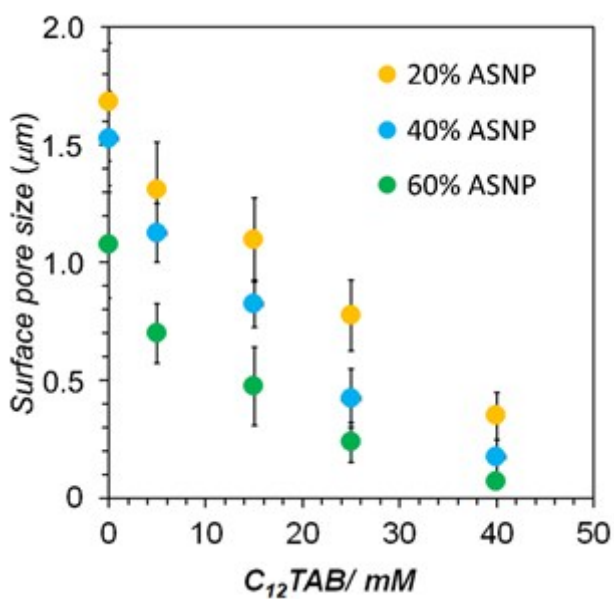
Hence, the absence of interfacial arrest at the internal regions of the bijel fibers - where the water component primarily partitions to – results in hollow fibers. Though undesired, this could be a novel route to fabricate non-bore-fluid bijel hollow-fiber membranes.



**Supplementary Figure 4:** Scanning Electron Micrographs (SEM) of the resulting structures formed by the direct addition of  $C_{16}TAB$  to the ternary mixtures prepared with acrylate silica nanoparticles. In the SEM, the oil domains are polymerized (indicated as gray), whereas the water domains are non-polymerized and subsequently dried up (indicated as dark). The cross sections of the fibers show the presence of nucleated water in oil droplets. At very high surfactant concentrations, fibers fail to form. Instead, oil in water droplets are formed (as observed for the 21 mM  $C_{16}TAB$  column), and even further, water-in-oil-in-water droplets are formed for the high acrylate density (60%-ASNP).

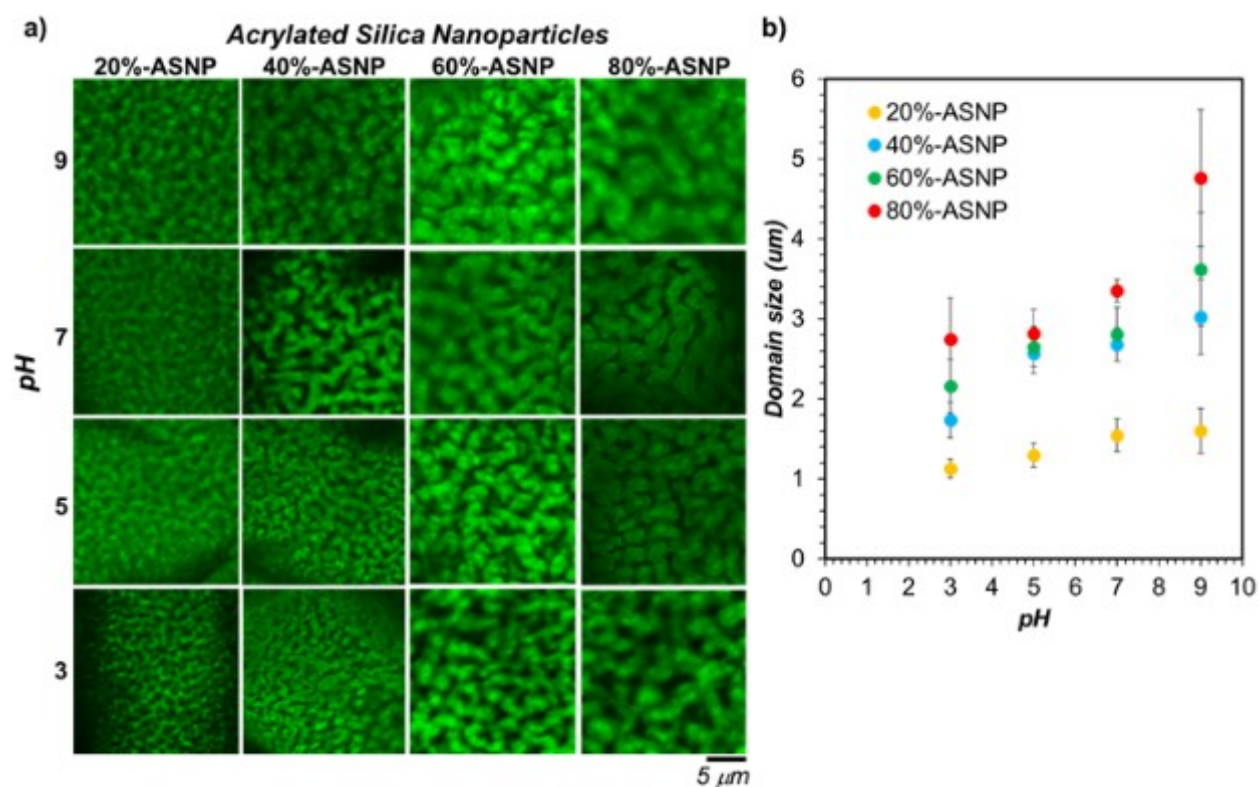
## Supplementary Note 5: Surface pore and Domain size characterization of ASNP-STrIPs bijels

In the previous reports of STriPS bijels where bare silica nanoparticles interacting with  $C_{16}$ TAB was used to fabricate bijel fibers, surface pore sizes ranging about 1  $\mu\text{m}$  to 5  $\mu\text{m}$  was measured where it was observed that surface pore sizes decreased with increasing surfactant concentration.<sup>2,3</sup> In this report where acrylate particles were used, not only does the surface pore sizes decrease with an increase in surfactant ( $C_{12}$ TAB) concentration, but also with an increase in the density of acrylate groups. It is however worth noting that the surface pores of ASNP-bijels are relatively smaller ( $< 2 \mu\text{m}$ ) (see supplementary Figure 5) compared to previous reports,<sup>2,3</sup> because of the extensive aggregation of hydrophobic acrylate particles at the bijel surface.



**Supplementary Figure 5:** ASNP-STriPS bijel fiber surface pore characterization in dependence of surfactant ( $C_{12}$ TAB) concentration. The surface pore sizes of ASNP bijel fibers decrease with an increase in surfactant concentration, as well as with the degree of particle acrylation.

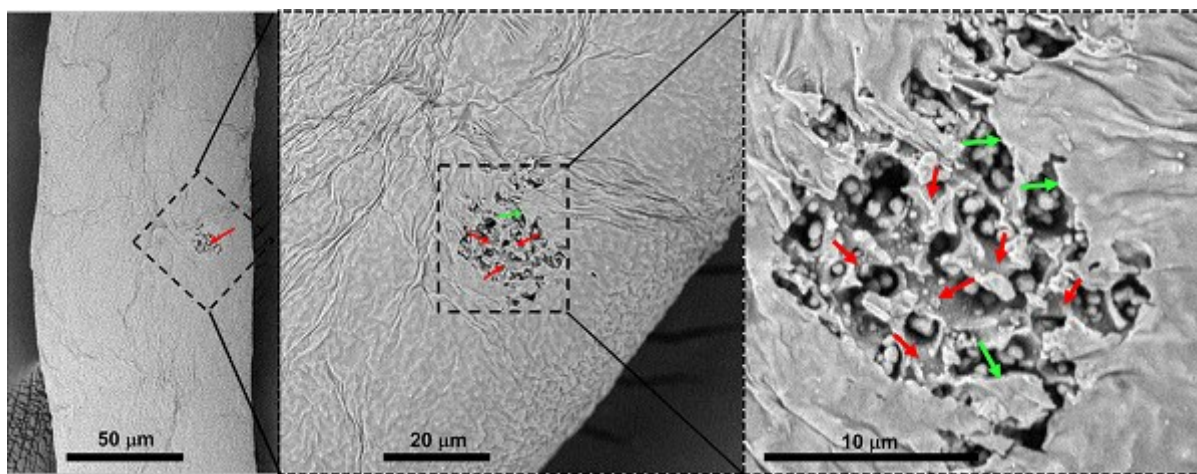
Moreover, we observe that the oil domain sizes of the ASNP-STriPS bijels (measured at the surface) increase with an increase in the degree of acrylation as well as pH (Supplementary Figure 6a). We believe that this is due to the increased partitioning of higher degrees of acrylate particles into the oil domains, hence, their accumulation in the hydrophobic component of the bijel, causing a corresponding increase in domain size. Additionally, the oil domain sizes increase with an increase in pH. This is likely due to the overall increase in the hydrophobicity of acrylate particles as a result of increased adsorption of cationic surfactant ( $C_{16}TAB$ ) on the increased negative charges on the particle surface.<sup>4</sup> Hence, the oil-domain sizes increase as observed in Supplementary Figure 6a, which is characterized and also shown in the graphical plot in 6b.



**Supplementary Figure 6:** Bijel surface domain size characterization of ASNP-STriPS bijels. a) Confocal laser scanning micrographs of the surface of STriPS bijels fabricated with varying degrees of acrylate particles (20%, 40%, 60%, and 80%-ASNPs) and at different pH conditions (decreasing from top to bottom). b) Corresponding bijel surface oil domain size characterization of the confocal images in (a).

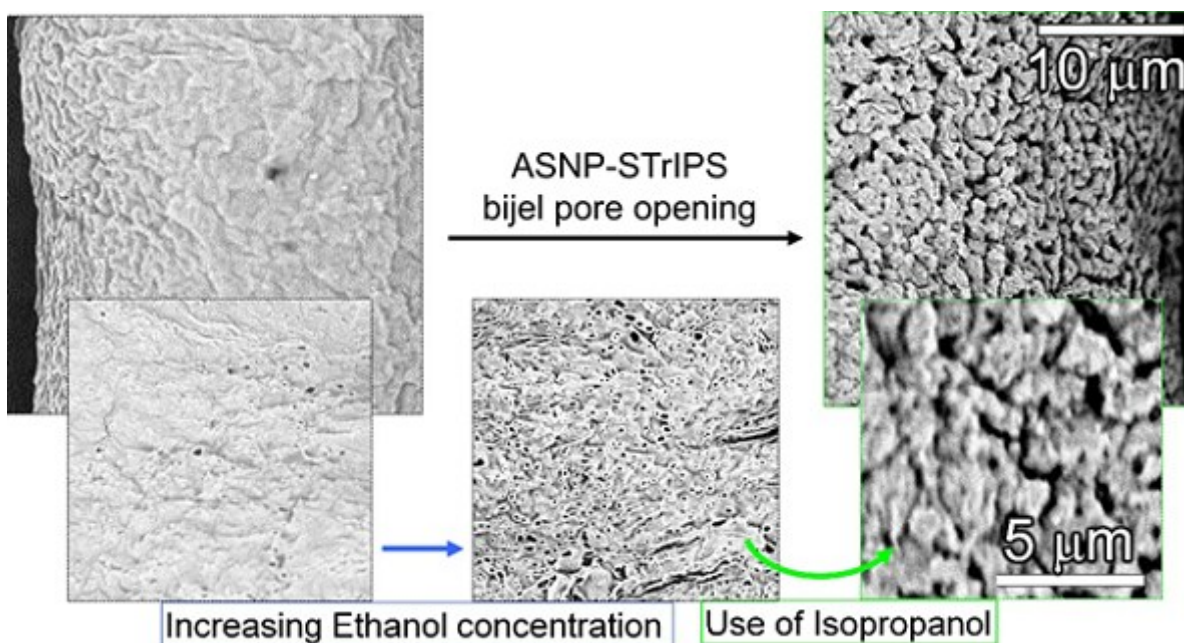
## Supplementary Note 6: Control of excess nanoparticles at the surface of ASNP-STrIPS bijels

During STrIPS bijel fabrication, excess nanoparticles aggregate at the surface of the water pores and in effect, covers the underlying bicontinuous structures.<sup>2,3</sup> Similarly, scanning electron micrographs (SEM) of STrIPS bijels fabricated with acrylated silica nanoparticles show that a thin sheet of aggregated nanoparticles cover the surface of the bijel fiber (Supplementary Figure 7).



**Supplementary Figure 7:** SEM images of 20%-ASNP STrIPS bijel fiber showing the aggregation of nanoparticles at the surface. The red arrow (in the left figure) show an exposed underlying patch of bicontinuous structures which is made more visible in the magnified images (on the right), whereas, the green arrows show the thin film of aggregated nanoparticles on the bijel-fiber surface.

As previously reported, the thin layer of aggregated nanoparticles was partially dispersed when a fraction of ethanol (5 - 20 %) was included in the continuous water phase.<sup>3</sup> In our case where hydrophobic acrylate particles were used, even ethanol concentrations of up to 20% v/v was not capable of effectively dispersing the surface-aggregated acrylate particles. Hence, a more apolar solvent, isopropanol (10% v/v) was needed to obtain bijel surface pore opening for ASNP-STrIPS bijels (see Supplementary Figure 8).

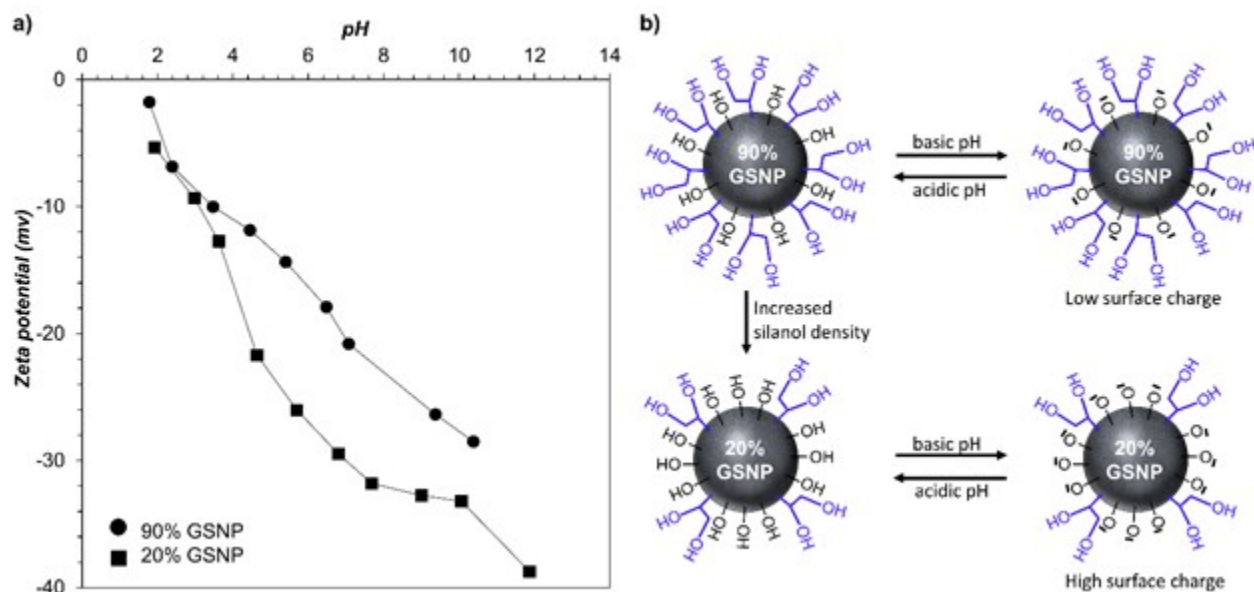


**Supplementary Figure 8:** Pore size control of ASNPs-STrIPS bijel. Effective pore opening is observed when isopropanol (10v/v %), instead of ethanol is used during the fabrication of ASNPs-STrIPS bijel fibers. Unlike bare silica nanoparticles, acrylate particles are highly hydrophobic and hence, the surface particle aggregation is more pronounced. The addition of ethanol is not effective in dispersing the aggregated particles. Isopropanol is more effective in dispersing the surface aggregated acrylate particles, resulting in effective surface pore opening.

### **Supplementary Note 7: Surface Charge Measurements of glycerol functionalized silica nanoparticles particles.**

Zeta potential measurements conducted on silica nanoparticles having varying degrees of glycerol functional groups (20% and 90%) show that the density of the functional groups affects the electrophoretic mobility, hence, the measured surface charge. High degrees of functional groups (e.g. 90% glycerol) covering the surface of silica nanoparticles correspond to a low degree of remaining silanol groups (~10% Si-OH), and vice versa. Supplementary Figure 9a shows the zeta potential measurements on silica nanoparticles covered with 20% and 90% glycerol groups, and in dependence of pH. Comparatively, 20%-GSNPs show an increased response to pH alterations, reflecting a more pronounced dissociation of a higher fraction of available silanol

groups, hence a higher magnitude of measured negative surface charges. On the other hand, 90%-GSNPs have relatively less amount of remaining silanol groups resulting in a relatively lower magnitude of surface charges. (see schematic in supplementary Figure 9b).

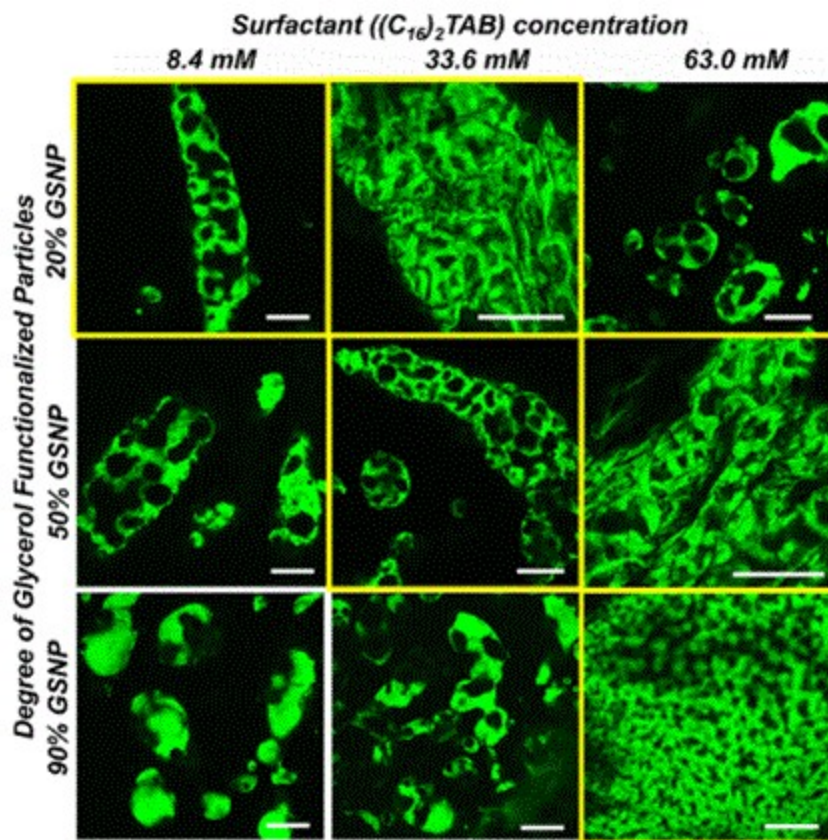


**Supplementary Figure 9:** Surface charge measurements of Glycerol functionalized particles. **(a)** Results of zeta potential measurements of 2wt % aqueous dispersions of glycerol functionalized silica nanoparticles (20% and 90% -GSNPs) at different conditions of pH. For a characteristic pH variation (for example, from 3 to 8), the change in magnitude of zeta potential values measured for 20%-GSNPs is relatively higher (~ 22 mV), as compared to a lower magnitude change (~ 13 mV) measured for 90%-GSNPs. This is attributed to the lesser density of remaining silanol groups available for charge dissociation in the case where the functional group density is high. **(b)** Schematic depiction glycerol functionalized silica nanoparticles and their response to pH. At the same basic pH for both 20% and 90% GSNPs, a greater number of negative surface charges are measured for the lesser degree of functional groups.

### Supplementary Note 8: Effect of glycerol density and surfactant concentration on STRIPS bijel formation.

The hydrophilic property of glycerol functionalized particles is expected to increase in relation to an increase in the degree of glycerol groups covering the surface of the silica nanoparticles. The abundance of hydroxyl groups on higher degrees of glycerol (e.g. 90%-GSNP) requires the use of higher concentrations (63 mM) of the cationic surfactant, dihexadecyldimethylammonium

bromide ( $(C_{16})_2TAB$ ) in order to stabilize bijels (see Supplementary Figure 10). Such high surfactant concentrations are required to counter the extreme hydrophilic effect imparted by the high glycerol density. On the other hand, when a similar surfactant concentration (63mM,  $(C_{16})_2TAB$ ) is used on 20%-GSNP, bijels fail to form. Instead, water-in-oil emulsion droplets are formed, depicting particles that have been extensively hydrophobized by the surfactant adsorption. However, the stabilization of viscoelastic structures in the same, depicts the presence of interfacially jammed particles. In effect, a relatively less surfactant concentration (8.4 mM,  $(C_{16})_2TAB$ ) is enough to stabilize bijels made with 20%-GSNPs. For the 50%-GSNPs, it wasn't until surfactant ( $(C_{16})_2TAB$ ) concentrations reached 12.6 mM that bijel-like structures formed (see Fig. 5 in main text). Further increase in surfactant concentrations up to 63 mM still resulted in bijel

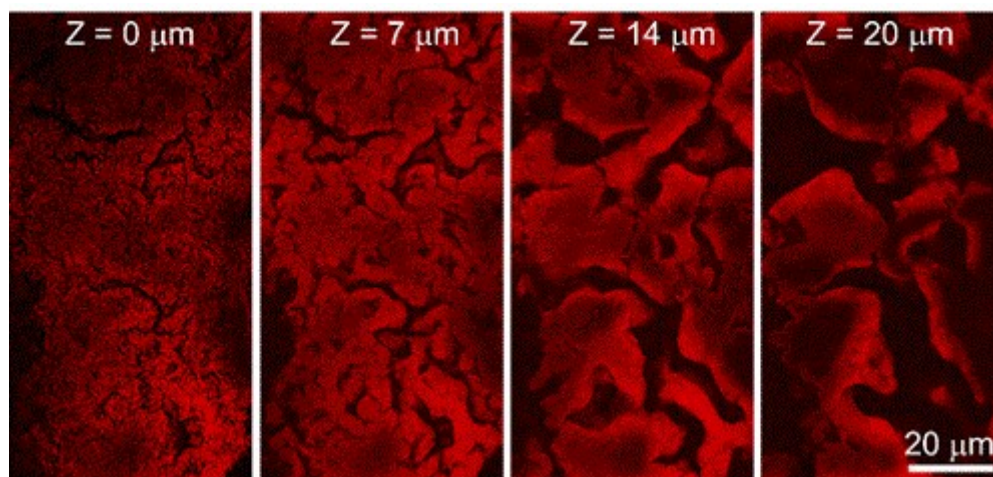


**Supplementary Figure 10:** Confocal laser scanning micrographs of emulsion structures stabilized with hydrophilic glycerol functionalized silica nanoparticles and surfactant  $(C_{16})_2TAB$ . The emulsion structures are fabricated with glycerol particles of varying densities (20%, 50% and 90% - GSNPs) and at varying surfactant ( $(C_{16})_2TAB$ ) concentrations. *First column:* At low surfactant concentrations (8.4 mM,  $(C_{16})_2TAB$ ), the double chain surfactants form bijels only at low glycerol densities (20%-GSNP). *Second column:* When the surfactant concentration is increased to 33.6 mM, bijel structures are formed for both 20% and 50% GSNPs. *Third row:* Further increase in surfactant concentration to 63mM, leads to formation of water in oil emulsions for 20%-GSNP, whereas bijel structures are formed for 50% and 90% GSNPs. The oil domains are color-coded as green, whereas the water domains are coded as black. Scale bar 50  $\mu$ m.

structures (Supplementary Figure 10).

### Supplementary Note 9: Dye adsorption on crosslinked bijel scaffolds after fluid remixing

The crosslinked silica nanoparticles scaffold remaining after fluid remixing is visualized under confocal microscopy by rendering the silica particles fluorescent. To realize this, we first increase the pH of the nanoparticle scaffold to generate negative charges on their surface. Subsequently, positively charged Rhodamine (110) dye is introduced to render the crosslinked particles fluorescent, which enable us to visualize the remaining scaffold under confocal microscopy (Supplementary Figure 11).



**Supplementary Figure 11:** Confocal Laser Scanning Micrographs of fluorescent crosslinked STRIPS bijels after fluid remixing. To cause fluid remixing in the crosslinked bijel, ethanol is added which removes both fluids (oil and water) from the bicontinuous domains, but the nanoparticle crosslinked scaffold remains (Figure 6d). Water is then added multiple times to dilute the ethanol and also to introduce scaffold to an aqueous bath for pH adjustments. A basic buffer solution (1 M  $\text{NaH}_2\text{PO}_4$ ) is introduced to the aqueous bath to adjust the pH to 12, which leads to the dissociation of the remaining silanol groups on the surface of the crosslinked glycerol silica nanoparticles. Excess basic water is removed by washing with DI water multiple times, after which the positively charged Rhodamine (110) dye is introduced. Prior to the addition of the dye, the entire crosslinked bijel scaffold remains dark under the confocal microscope is made visible when the dye adsorbs onto the silica particle scaffold. The bijel scaffold deflated upon fluid remixing, hence the observed shifting the equatorial axis (from  $\sim 40 \mu\text{m}$  to  $20 \mu\text{m}$ ).

### References

- 1 E. F. Vansant, P. Van Der Voort and K. C. Vrancken, *Characterization and chemical modification of the silica surface*, Elsevier, 1995, vol. 93.
- 2 M. F. Haase, K. J. Stebe and D. Lee, *Advanced Materials*, 2015, **27**, 7065–7071.
- 3 M. F. Haase, H. Jeon, N. Hough, J. H. Kim, K. J. Stebe and D. Lee, *Nature Communications*,

2017, **8**, 1234.

4 T. G. Anjali and M. G. Basavaraj, *Langmuir*, 2018, **34**, 13312–13321.